Supporting information

Gold nanostars: surfactant-free synthesis, 3-D modelling, and two-photon luminescence imaging

Hsiangkuo Yuan[1§], Christopher G Khoury[1§], Hanjun Hwang[1], Christy M Wilson[2], Gerald A Grant[2] and Tuan Vo-Dinh[1,3,4] *

[1] Department of Biomedical Engineering, Duke University, Durham, NC 27708, USA
[2] Department of Surgery, Division of Neurosurgery, Duke University Medical Center, Durham, NC.
[3] Department of Chemistry, Duke University, Durham, NC 27708, USA
[4] Fitzpatrick Institute for Photonics, Duke University, Durham, NC 27708, USA
[§] These authors contributed equally

* Email: tuan.vodinh@duke.edu

Surfactant-free synthesis and plasmon tunability of nanostars

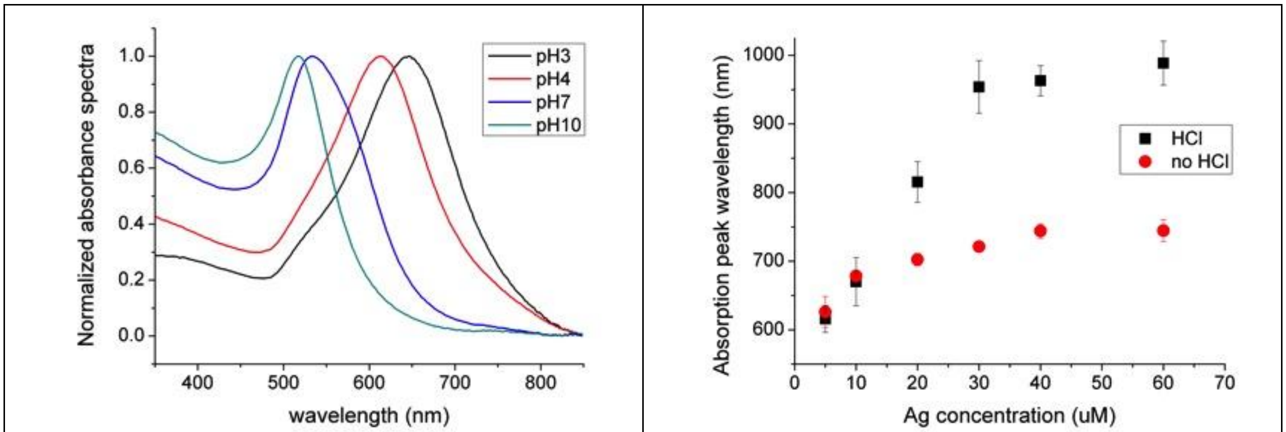

Figure 1: pH effect on the growth of nanostars. (left) Normalized spectra (pH 3~10: brown, red, blue, green line) of nanostars synthesized under different pH buffer (20 mM). The plasmon red-shifted the most under an acidic environment. (right) Plasmon peak position of nanostars, from different Ag^{+} concentrations, synthesized with (black square) and without (red circle) the addition of 10 µl 1N HCl.

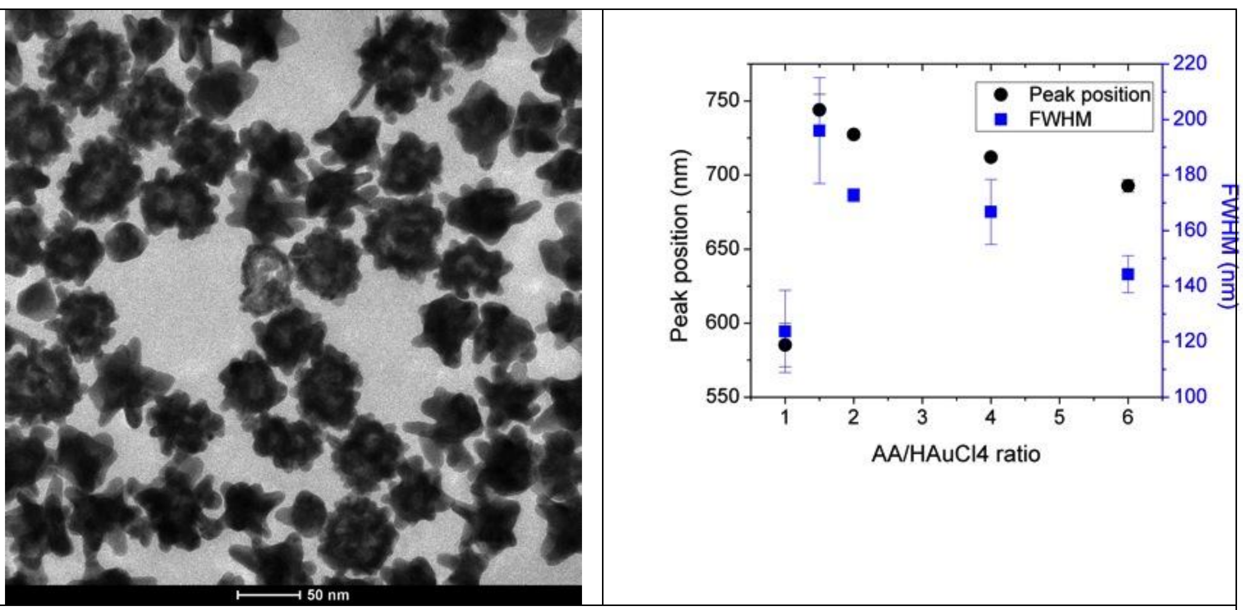

Figure 2: AA/$HAuCl_4$ ratio effect on the growth of nanostars. (left) TEM image of particles formed at AA/$HAuCl_4$ ratio of 6. Particles were flower-shape instead of star-shape. (right) Plasmon peak position (black circle) and FWHM (blue square) of the absorbance spectra on nanostar synthesized by different AA/$HAuCl_4$ ratio. Ascorbic acid at 1.5~2x molar ratio to $HAuCl_4$ resulted in the most red-shifted plasmon peak position. As previously shown, 1x and higher (>3x) ratio leads to the formation of polydisperse particles and short-branched nanoflowers respectively [2, 3].

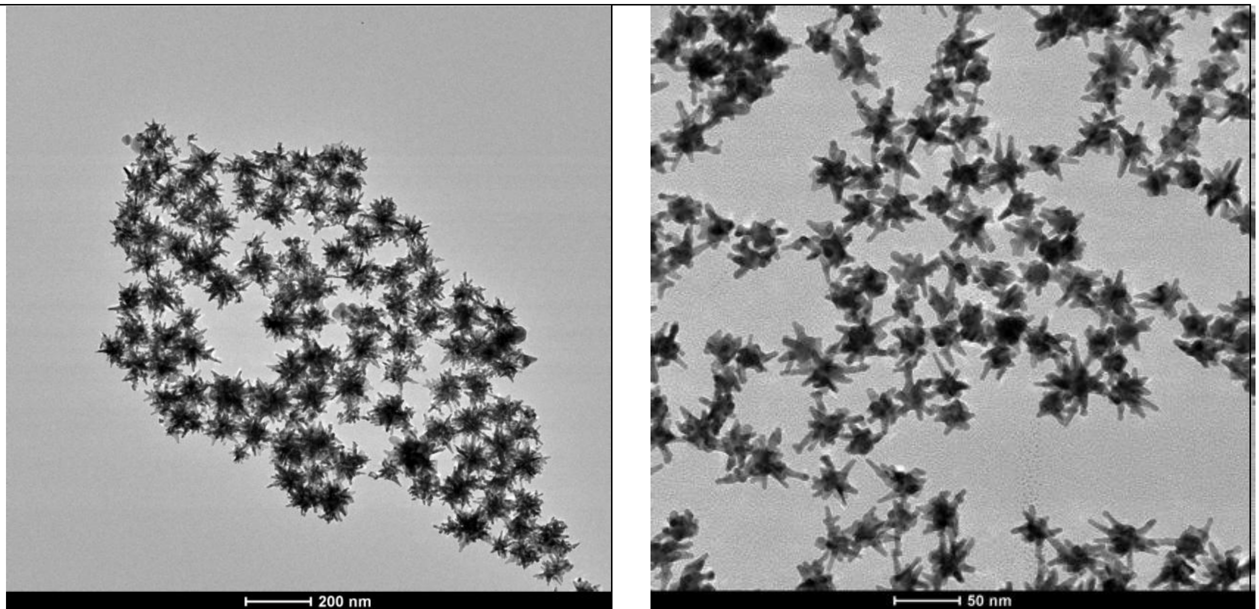

Figure 3: Effect of the seed amount on growth of nanostars. TEM images of nanostars made from no seed (left) and 400 μl (right) of seeds under 30 μM of silver nitrate. The average size was larger than 100 nm without seed and less than 50nm with 4-fold amount of seeds.

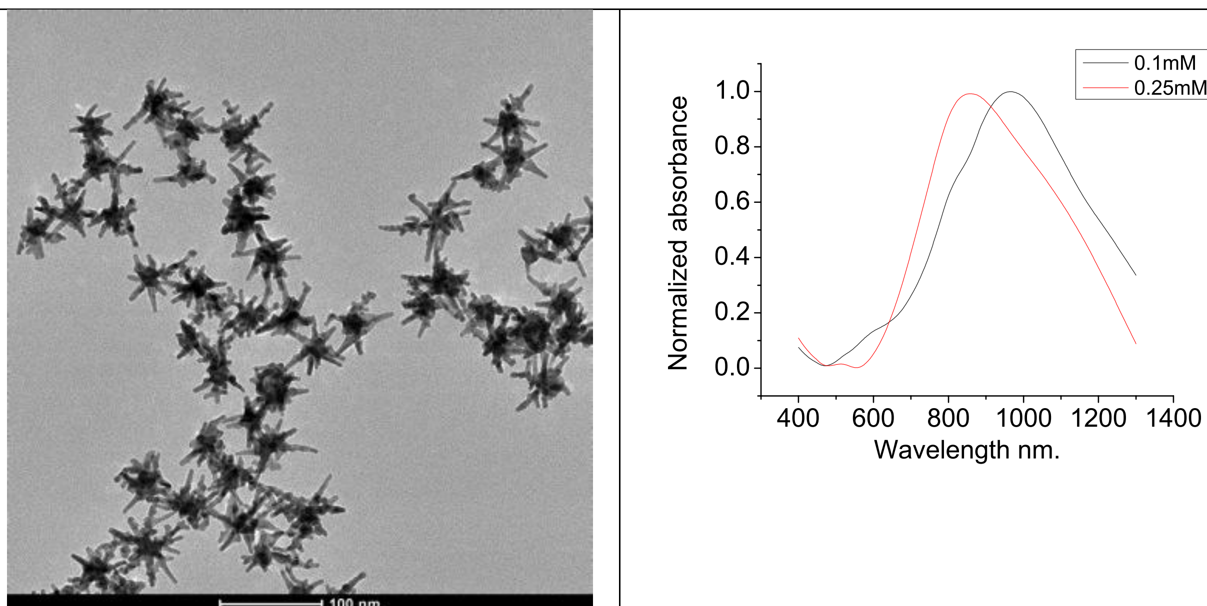

Figure 4: Effect of $HAuCl_4$ concentration on growth of nanostar. (left) TEM image of nanostars made from 0.1 mM $HAuCl_4$ and 20 μM of $AgNO_3$. The core size is roughly 10 nm smaller and the branches are thinner than the one made from 0.25 mM $HAuCl_4$. (right) Normalized absorbance spectra of nanostars made from 0.1 mM (grey line) and 0.25 mM (red line) $HAuCl_4$. Nanostars with smaller core has more red-shifted plasmon spectrum.

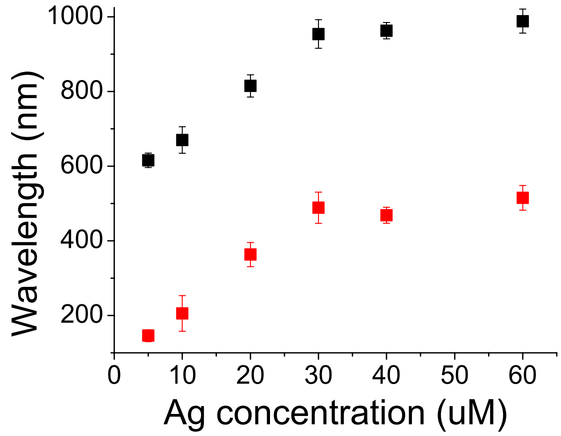

Figure 5. The spectral progression of plasmon peak (black square) and FWHM (red square) of nanostars formed under different Ag^+ concentrations.

Polarization-averaged 3-D nanostar modelling

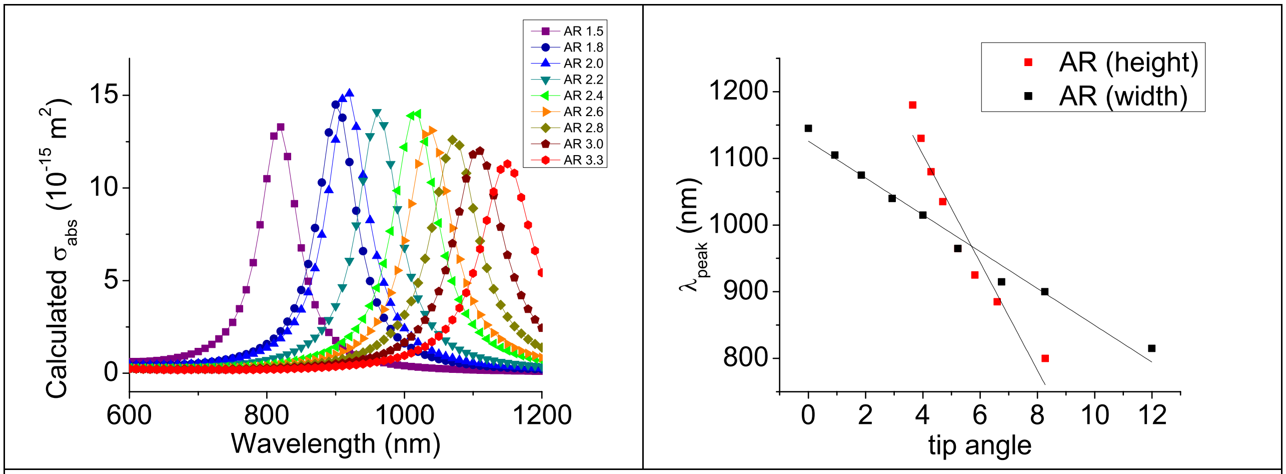

Figure 6. (left) The scatter plots of polarization-averaged absorption against aspect ratio (AR) tuned by branch base width while keeping the branch height, core/tip diameter and branch number constant. (right) Relationship between plasmon peak position and tip angle tuned by branch height (red, R^2=0.928) and base width (black, R^2=0.979).

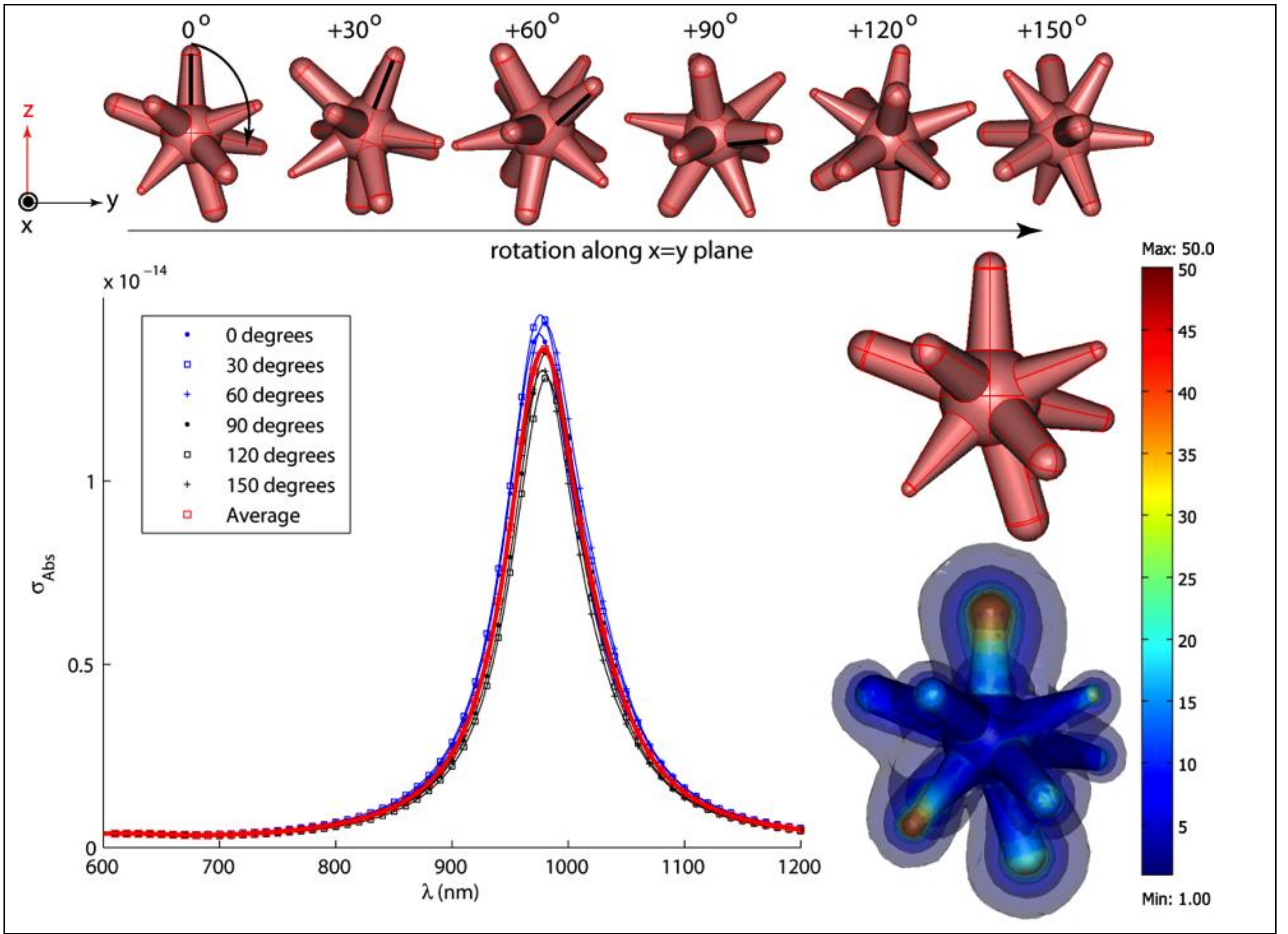

Figure 7. Polarization-averaged absorption spectra of nanostar of 10 branch with various tip radius of curvature but the same approximate aspect ratio (Table below). The 3-D spatial solution of $|E_z|$ are evaluated at λ=960nm.

Tip radius of curvature of 10 branches

Branch #	Length (nm)	Base Width (nm)	Angle (^{o})	Tip radius (nm)	Aspect Ratio (L/W)
1	23.4	5.0	1.0	4.72	2.34
2	23.0	5.0	2.0	4.40	2.30
3	22.7	5.0	3.0	4.08	2.27
4	22.4	5.0	4.0	3.75	2.24
5*	22.0	5.0	5.0	3.35	2.20
6	21.8	5.0	6.0	3.10	2.18
7	21.4	5.0	7.0	2.75	2.14
8	21.1	5.0	8.0	2.44	2.11
9	20.8	5.0	9.0	2.10	2.08
10	20.4	5.0	10.0	1.77	2.04

***original S30 branch dimensions**

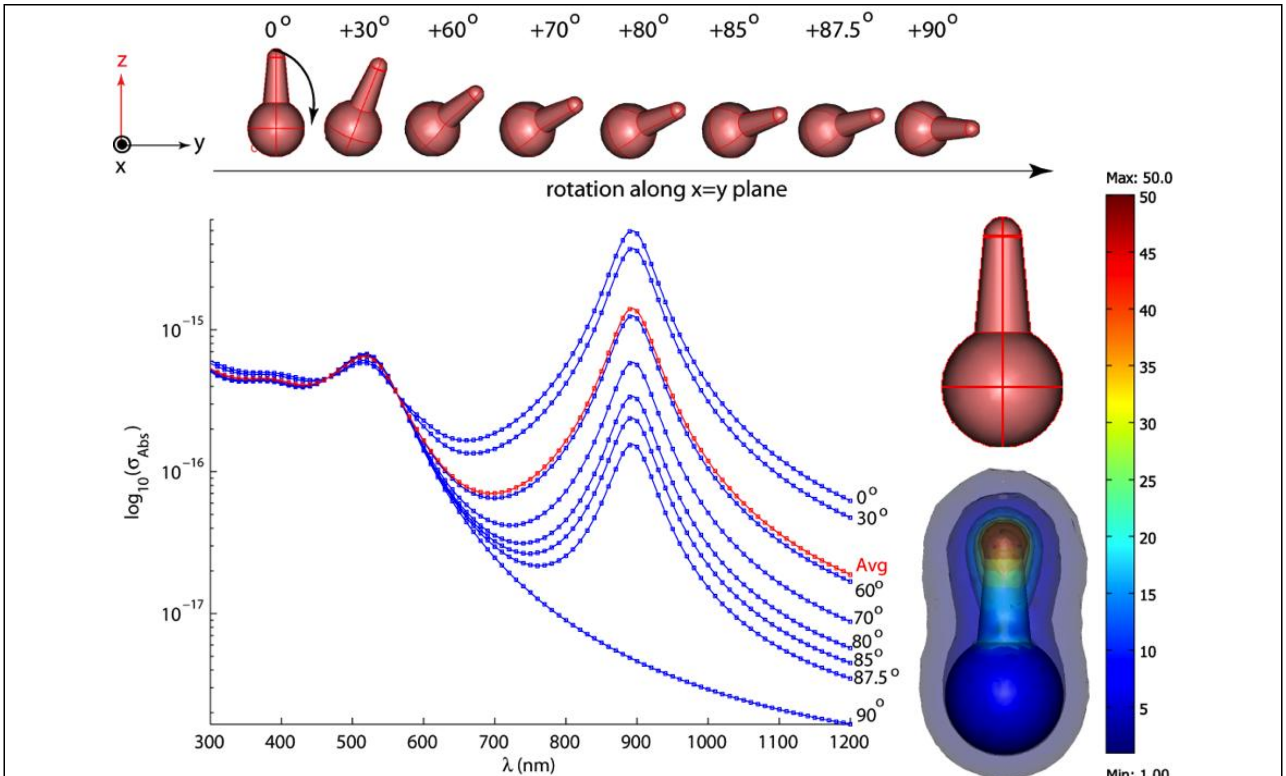

Figure 8: Numerically solved polarization-averaged absorption spectra for a single-branched nanostar. The 3-D spatial solutions of $|E_z|$ are evaluated at λ=960nm.

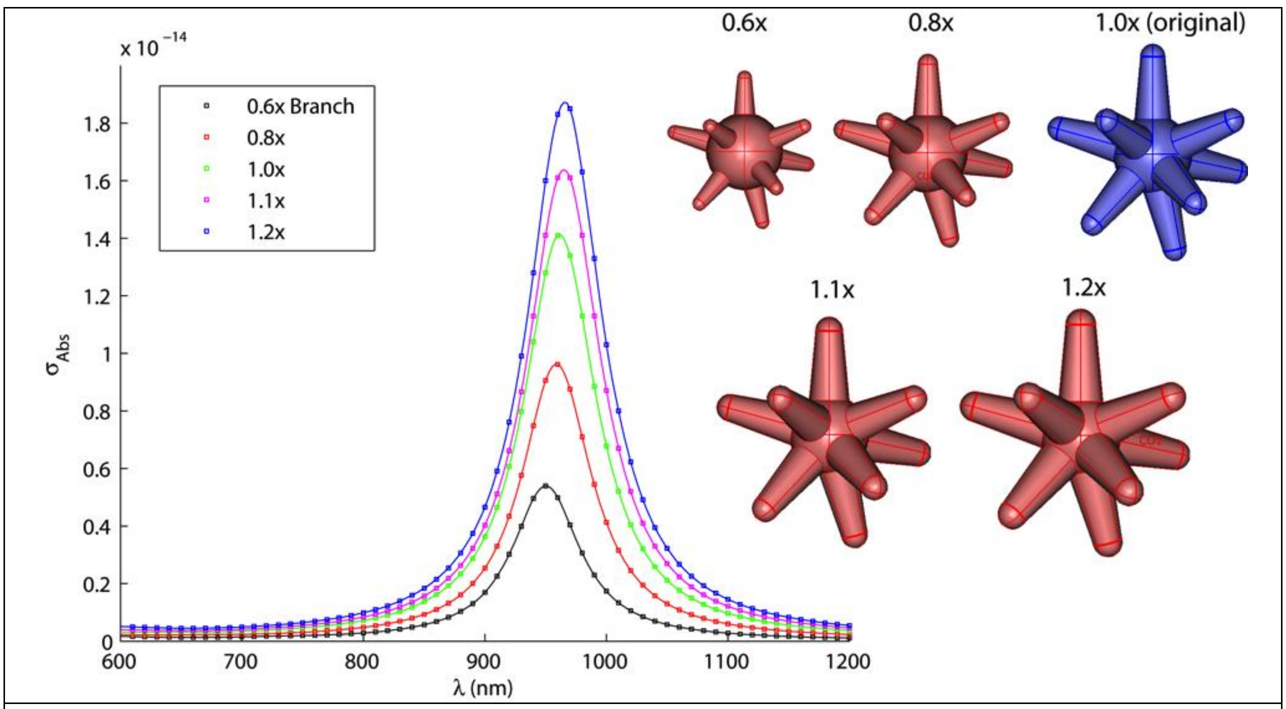

Figure 9. Polarization-averaged absorption spectra as a function of branch length (keeping the aspect ratio constant) of S30 nanostar. Longer branch length results in higher peak intensity but no significant plasmon shift.

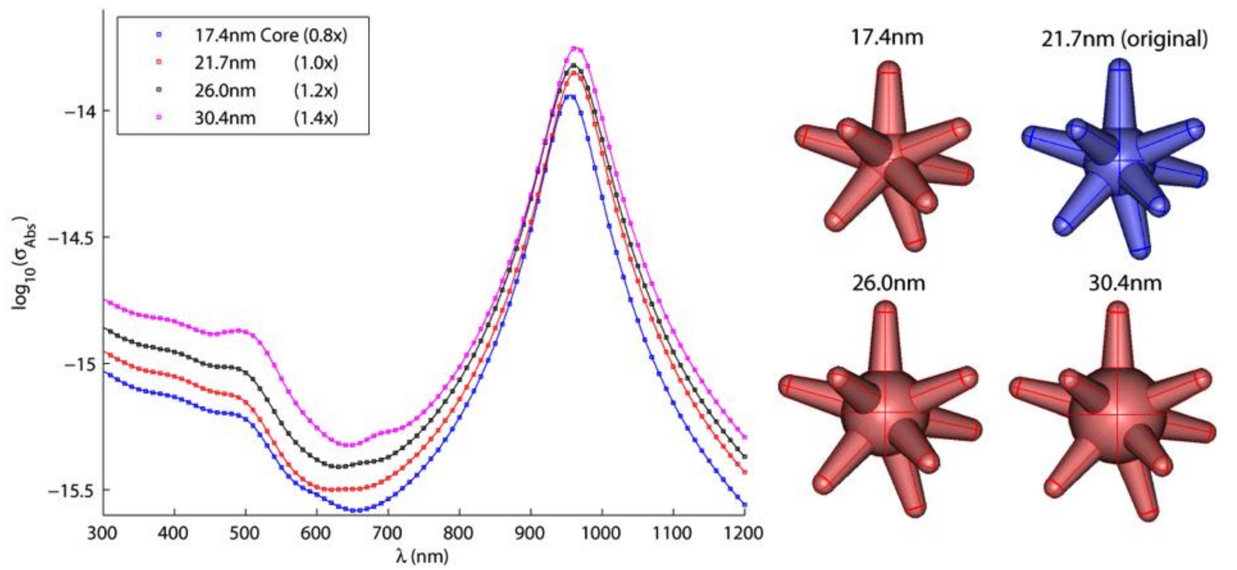

Figure 10: Absorption spectra as a function of nanostar core diameter. The core diameter affects primarily the plasmon near 520 nm.

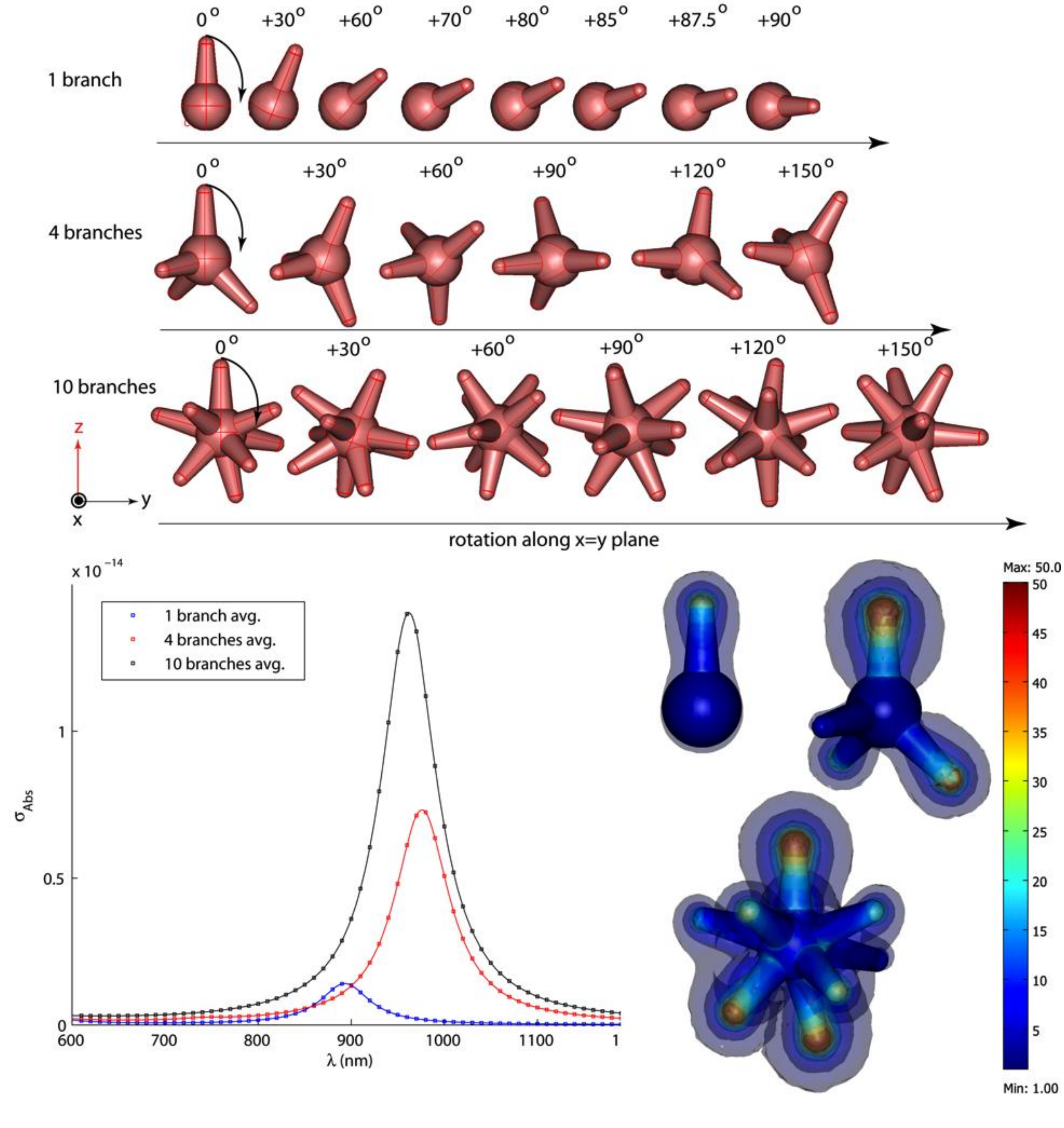

Figure 11: Polarization-averaged absorption spectra as a function of number of branches of S30 nanostar. The 3-D spatial solutions of $|E_z|$ are evaluated at λ=960nm. Plasmon peaks are similar for nanostars with 4 and 10 but not 2 branches.

Table 1. Structural features of nanostars produced under different Ag^+ concentrations

Ag^+ (μM)	Hydrodynamic size (nm)	Core diameter (nm)	Branch length (nm)	Branch base width (nm)	Tip diameter (nm)	Branch number	Estimated surface area via simulation (nm^2)
5	50±24	28.4±2.6	13.1±5.0	18.5±3.1	11.1±1.5	4.2±1.9	3416
10	51±21	28.2±3.1	14.7±4.3	16.4±3.3	9.4±1.4	6.4±1.4	4665
20	59±21	23.7±2.4	19.0±5.1	13.5±2.4	7.8±1.3	7.8±1.1	5202
30	67±24	21.7±3.6	20.9±5.1	10.1±2.0	6.5±1.4	9.9±2.4	5924

Hydrodynamic sizes were obtained using the NanoSight measurements. Other structural features were measured from TEM images manually using ImageJ software. Surface area was calculated from the simulation geometry.

Nanostars two-photon photoluminescence

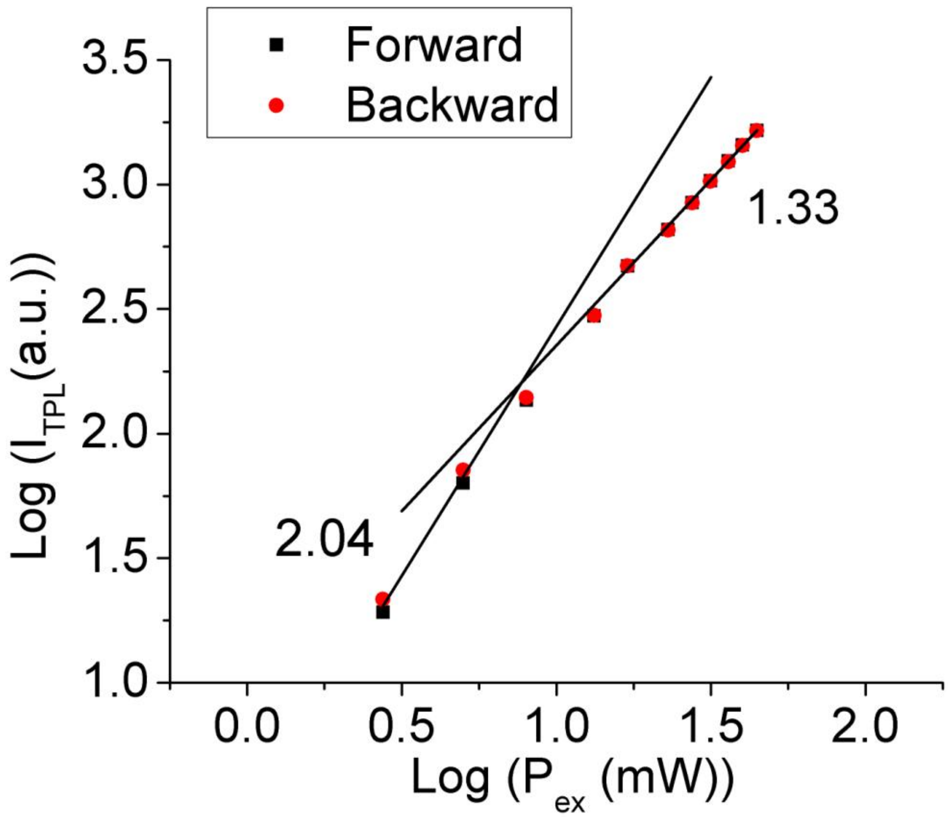

Figure 12. Dependence of the TPL intensity (I_{TPL}) on the laser power. The power adjusted by increasing (forward) or decreasing (backward) between 3~45 mW. A transition from quadratic (2.04) to near linear (1.33) dependence was observed.

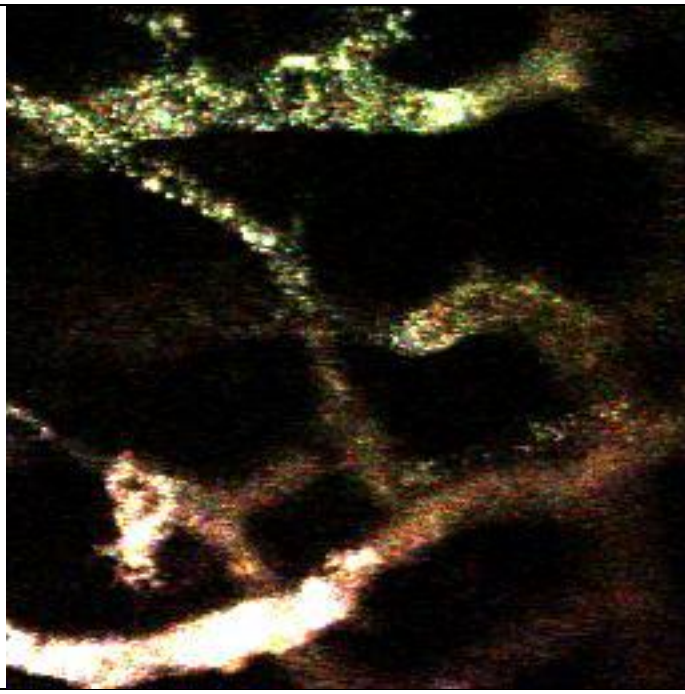

Movie 1. TPL imaging through dorsal window chamber 30 min after nanostars injection. The time-series was taken under 3% laser transmission at 2.3 frame per second (256 × 256 resolution) with a scanning area of 145 × 145 μm^2. The movie shows the flow of PEGylated gold nanostars in the blood vessel.

Reference:

1. Ji, X.; Song, X.; Li, J.; Bai, Y.; Yang, W.; Peng, X., Size control of gold nanocrystals in citrate reduction: The third role of citrate. *J. Am. Chem. Soc* **2007,** *129* (45), 13939-13948.
2. Ahmed, W.; Kooij, E.; Silfhout, A.; Poelsema, B., Controlling the morphology of multi-branched gold nanoparticles. *Nanotechnology* **2010,** *21*, 125605.
3. Kawamura, G.; Yang, Y.; Fukuda, K.; Nogami, M., Shape control synthesis of multi-branched gold nanoparticles. *Mater. Chem. Phys.* **2009,** *115* (1), 229-234.